East Asian Winter Monsoon, Arctic Oscillation, and East Asian Cold Surges

Song Yang[1], Yueqing Li[2], Tae-Won Park[3], and Chang-Hoi Ho[3]

[1]NOAA Climate Prediction Center, 5200 Auth Road, Camp Springs, Maryland 20746, USA
(Song.Yang@noaa.gov)
[2]Institute of Plateau Meteorology, China Meteorological Administration, Chengdu, China
[3]School of Earth and Environmental Sciences, Seoul National University, Seoul, Korea

Abstract

In this study, a dynamical index is constructed for the East Asian winter monsoon considering that the winter monsoon is a deep system and interacts with both tropical and extratropical systems. The index represents many important features of the monsoon including its strong relationships with surface air temperature, low-level meridional wind, Siberian high, East Asian trough, upper-tropospheric westerly jet streams, and Southeast Asian cold surges. It also depicts the relationships of the monsoon with the Arctic Oscillation (AO) and ENSO. The NCEP Climate Forecast System skillfully captures the variability of the winter monsoon index and the relationships of the monsoon with tropical and extratropical systems. The model is able to predict the monsoon in advance by 3 months. The East Asian cold surges, which are active in strong monsoon years and La Niña years and inactive in weak monsoon years and El Niño year, are closely related to the phase of AO. When the AO is in negative (positive) phase, the cold surges are of blocking (shortwave) type and are more (less) active.

Key words: East Asian winter monsoon, dynamical monsoon index, Arctic Oscillation, East Asian cold surges, and NCEP model

1. Introduction

Compared to the Asian summer monsoon, the East Asian winter monsoon (EAWM) has been studied less extensively. The EAWM produces large-scale northerly surges and temperature drops across East Asia and exerts a strong influence on the climate over remote regions. The variability of EAWM often causes substantial social and economic losses. The East Asian cold surges (EACS) lead to abrupt temperature drops with prevailing northerly wind related to strong cold advection along the edge of the Siberian high. They often cause heavy freezing precipitation and snowfall over East Asia and modulate the convective activity over the South China Sea.

Previous studies of EAWM and EACS mostly focus on their features at the lower troposphere and their relationships with high-latitude systems. In particular, features of the association between low-level winter monsoon flow and surface air temperature and the relationships between EACS as cold-air outbreaks and the Siberian high have been studied extensively.

In this paper, we define an index of EAWM based on the belief that the physical processes of both higher and lower latitudes, and at both lower and upper troposphere, should be considered to depict the variability of the winter monsoon (see Li and Yang (2010) for details). We discuss the associations of the index with large-scale monsoon processes and EACS activity. We also discuss the variability of the EACS and its relationships with the

Arctic Oscillation (AO) and other large-scale atmospheric processes (see Park et al. (2010) for details). Furthermore, we assess the skill of prediction of the EAWM by the NCEP Climate Forecast System (CFS).

2. East Asian winter monsoon and a dynamical index

Since surface meridional wind is one of the key components of EAWM, we first compute the December-January-February (DJF) correlation between 1000-mb meridional wind averaged over 25-50°N/100-145°E and grid-point 200-mb zonal wind, indicating that the meridional wind over East Asia is closely connected to the East Asian westerly jet stream and the zonal winds on its both sides. When the jet stream strengthens (weakens) and these zonal winds weaken (strengthen), the surface northerly wind over East Asia is stronger (weaker), meaning that the EAWM strengthens (weakens). The features shown in Fig. 1a can also be found in the first mode of Singular Value Decomposition analysis of 1000-mb meridional wind and 200-mb zonal wind.

Figure 1b shows the DJF correlation between the time series of eastern hemisphere SLP (EHSLP) and grid-point 200-mb zonal wind (illustrated by the shadings). (EHSLP is the time coefficient of the first EOF mode of SLP over 30-50ºN/0-180°E.) EHSLP is closely related to AO, but is more significantly correlated with EAWM than is AO. As in Fig. 1a, Fig. 1b shows a distinct

"positive-negative-positive" structure with three bands of maximum correlation associated with changes in the East Asian westerly jet stream. The figure also shows significant correlation between Niño3.4 index and the upper-tropospheric zonal wind (contours), in which a "positive-negative-positive" structure of three bands of maximum correlation appears clearly as well. When warm (cold) SST appears over the tropical central-eastern Pacific, the East Asian westerly jet stream is weak (strong) and the zonal winds on its two sides strengthen (weaken). Given the feature shown in Fig. 1a, the warm (cold) SST is associated with weak (strong) surface northerly wind over East Asia, and thus weak (strong) EAWM.

Based on the three-band structure revealed in Fig. 1, we define a monsoon index for EAWM as:

Li-Yang = $\{[U_{200}(30\text{-}35^{\circ}N/90\text{-}160^{\circ}E)\text{-}U_{200}(50\text{-}60^{\circ}N/70\text{-}170^{\circ}E)]+[U_{200}(30\text{-}35^{\circ}N/90\text{-}160^{\circ}E)\text{-}U_{200}(5^{\circ}S\text{-}10^{\circ}N/90\text{-}160^{\circ}E)]\}/2.$

The above dynamical monsoon index represents many important features of the winter monsoon including its strong relationships with surface air temperature, low-level meridional wind, Siberian high, East Asian trough, and upper-tropospheric westerly jet streams. In particular, the index is significantly correlated with the most dominant modes of EOF analysis of sea level pressure, lower and upper-tropospheric winds, and mid-tropospheric geopotential height. The index also depicts the relationships of the monsoon with AO and ENSO. Furthermore, Fig. 2 shows that the monsoon index is significantly correlated with the activity of Southeast Asian cold surges defined by Chang et al. (2005), who measured the cold surge activity by the number of days of cold surges.

The newly defined monsoon index possesses a large predictability in the NCEP CFS. The model captures many features of monsoon variability and related large-scale features in the Siberian high, East Asian trough, and lower and upper-tropospheric circulation, AO, and ENSO. The model is able to predict the winter monsoon in advance by 3 months. Table 1 compares the skill of prediction of several winter monsoon indices in the CFS in 0-month lead (LM0; using initial conditions in November-December), 1-month lead (LM1; using initial conditions in October-November), 2-month lead (LM2), and 3-month lead (LM3). It reveals that in the short leads (LM0 and LM1), the skill is similar between the current index (Li-Yang) and Jhun-Lee (2004). However, the current index is more predictable in the longer leads. Overall, it shows higher skill compared to other indices.

Table 1. Correlations between observed EAWM indices and CFS-predicted EAWM indices at various lead times. Values in bold, italic, and underlined significantly exceed the confidence level of 99.9%, 99%, and 95%, respectively. Insignificant values are not shown.

	LM0	LM1	LM2	LM3
Li-Yang	**0.86**	**0.69**	<u>0.48</u>	<u>0.50</u>
Jhun-Lee (2004)	**0.81**	**0.69**		
Sun-Li (1997)	**0.72**	*0.57*		
Yang-Lau-Kim (2002)	**0.65**	*0.53*		
Shi (1996)	*0.60*	<u>0.45</u>		

3. East Asian cold surges and Arctic Oscillation

Figure 3 shows the time evolutions of anomalies of height at 300 mb and 850 mb, vertical cross-sections of height and potential temperature, and 850-mb temperature and horizontal wind composited for 31 cold surges during positive AO. An upper-tropospheric ridge-trough-ridge pattern in northwest-southeast direction from central Russia to Japan is found with a westward tilt relative to that at lower troposphere, and it moves southeastward toward East Asia with expansion of the Siberian high (Figs. 3a–3c). The vertical structure (Figs. 3d–3f) clearly shows a growing baroclinic wave system with a westward tilt of height and an eastward tilt of potential temperature at the troposphere. In addition, an in-phase and equivalent structure over Lake Baikal on day +2 in Figs. 3c and 3f can be found. There are significant negative height anomalies over the polar region at both the troposphere (Figs. 3a–3c) and the stratosphere (Figs. 3d–3f). Compared to the features for all 332 cold surges analyzed (figure not shown), the large-scale sea level pressure pattern during positive AO shows weakening of the Siberian high and the Aleutian low, which is linked to a weakening of the anticyclone–cyclone couplet with a high near the Siberian high and a low near the southwest edge of the Aleutian low (Figs. 3a–3c). The extent and amplitude of the cold anomaly over East Asia are also smaller and the cold advection is associated with anomalous northwesterly flow, instead of anomalous northerly flow (Figs. 3g–3i). Because the anomalous cyclone over Japan is particularly weak, the effect of this northwesterly flow on cold advection is dominant and particularly important in the occurrence of cold surges (Figs. 3b and 3h). Nevertheless, the cold surges during

positive AO tend to be characterized by the shortwave train type and are generally the cold surges over East Asia.

Figure 4 shows features associated with 60 cold surges during negative AO. Strong positive and negative height anomalies are found near the subarctic region and over East Asia on day –2 (Fig. 4a). The positive anomalies (i.e. blockings) are almost barotropic and stationary during the occurrence and development stages of cold surges, whereas the negative anomalies (i.e. troughs) have a baroclinic structure of westward tilt with height, intensifying the trough and propagating southeastward slowly (Figs. 4a–4c). Coinciding with the positive-negative dipole anomalies in meridional direction that constitute blocking and trough, the unusual southwestward expansion of the Siberian high is clearly shown in Fig. 4b. In Figs. 4a–4c, the expanding Siberian high forms strong anticyclone-cyclone couplet with negative height anomaly over Korea and Japan, which seems to strengthen the Aleutian low shown in sea level pressure during negative AO. Northeasterly flow appears over the entire East Asian seaboard along the couplet (Figs. 4g–4i). In contrast to those during positive AO shown in Fig. 3, the cold surges during negative AO are stronger due to the strong couplet structure, and thus the wide-spread and severe cold anomalies over East Asia are more evident (Figs. 4g–4i). In the vertical structure of blocking-type cold surges along the dipole anomalies, the maximum and minimum height anomalies are found at levels of about 20 mb and 300 mb, respectively (Figs. 4d–4f). During the occurrence and development stages of cold surges, stratospheric signals related to the blocking centered at the mid-stratosphere propagate downward into the troposphere, while the trough centered at the tropopause amplifies. The influence of this downward propagation of polar blocking related to negative AO suggests a stratospheric modulation on tropospheric circulation by the downward propagation of AO signals.

4. References

Chang, C.-P., P. A. Harr, and H.-J. Chen, 2005: Synoptic disturbances over the equatorial South China Sea and western maritime continent during boreal winter. *Mon. Wea. Rev.,* **133,** 489-503.

Jhun, J., and E. Lee, 2004: A new East Asian winter monsoon index and associated characteristics of the winter monsoon. *J. Climate,* **17,** 711-726.

Li, Y., and S. Yang, 2010: A dynamical index for the East Asian winter monsoon. *J. Climate,* in press.

Park, T.-W., C.-H. Ho, and S. Yang, 2010: Relationship between Arctic Oscillation on cold surges over East Asia. *J. Climate,* conditionally accepted.

Shi, N., 1996: Features of the East Asian winter monsoon intensity on multiple time scale in recent 40 years and their relation to climate. *Quart. J. Appl. Meteor.,* **7,** 175-181 (in Chinese).

Sun, B.-M., and C.-Y. Li, 1997: Relationship between the disturbances of East Asian trough and tropical convective activity in boreal winter. *Chinese Sci. Bull.,* **42,** 500-504 (in Chinese).

Yang, S., K.-M. Lau, and K.-M. Kim, 2002: Variations of the East Asian jet stream and Asian-Pacific-American winter climate anomalies. *J. Climate,* **15,** 306-325.
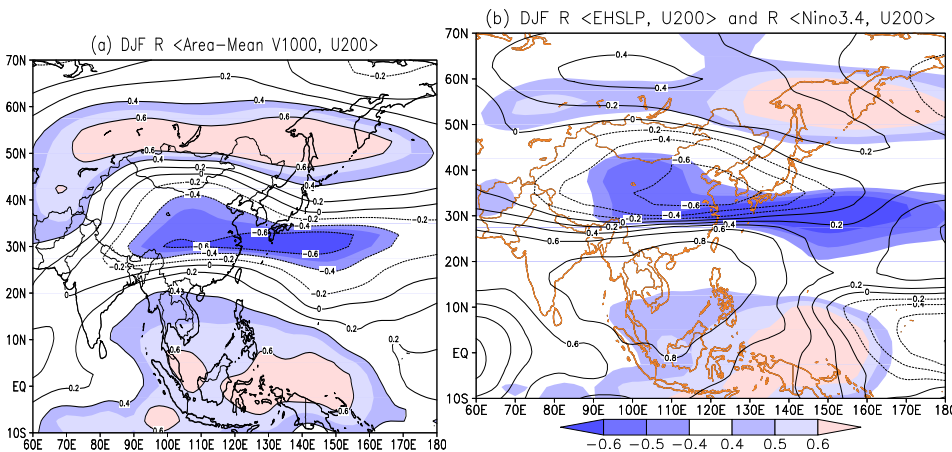
Fig. 1. (a) Correlation between area-averaged 1000-mb meridional wind (over 25-50°N/100-145°E) and grid-point 200-mb zonal wind for 1982-2006. (b) Correlation between EHSLP and grid-point 200-mb zonal wind (shadings) and between Niño3.4 SST and 200-mb zonal wind (contours). The threshold values of the 95%, 99%, and 99.9% confidence levels of significance are 0.40, 0.51, and 0.62, respectively.
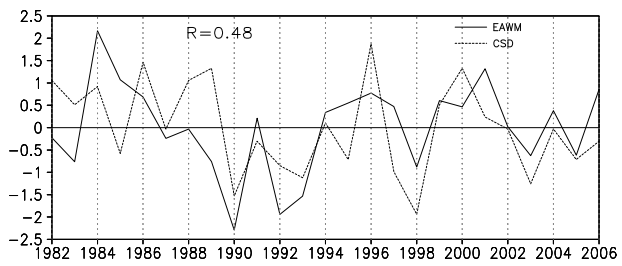
Fig. 2. Normalized time series of Li-Yang index (solid line) and Southeast Asian cold-surge index (Chang et al. 2005; dotted line).
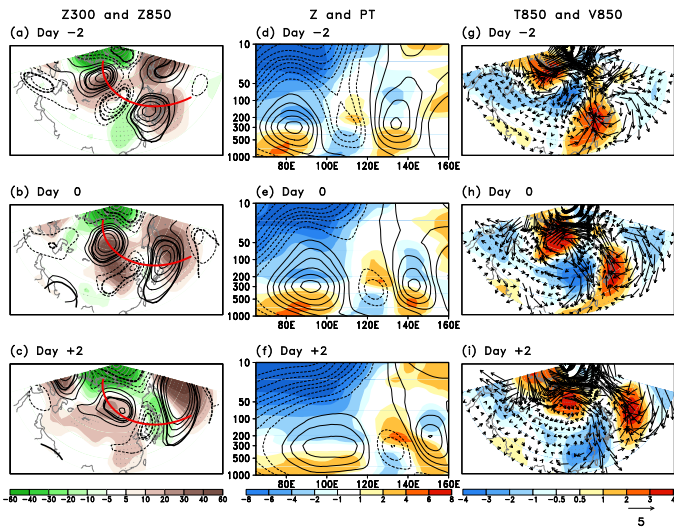
Fig. 3. Composite anomalies of (a)–(c) geopotential height at 300-mb (contours; in interval of 20 m, significant values at the 95% confidence level are represented by thick lines) and 850-mb (shadings; significant values at the 95% confidence level are represented by grey dots); (d)–(f) vertical cross-sections of geopotential height (contours; in interval of 20 m) and potential temperature (shadings) along the red thick lines in (a)–(c); and (g)–(i) temperature (shadings; significant values at the 95% confidence level are represented by grey dots) and winds (vectors) at 850-mb during day –2 to day +2 relative to 31 cold-surge occurrences during positive AO.
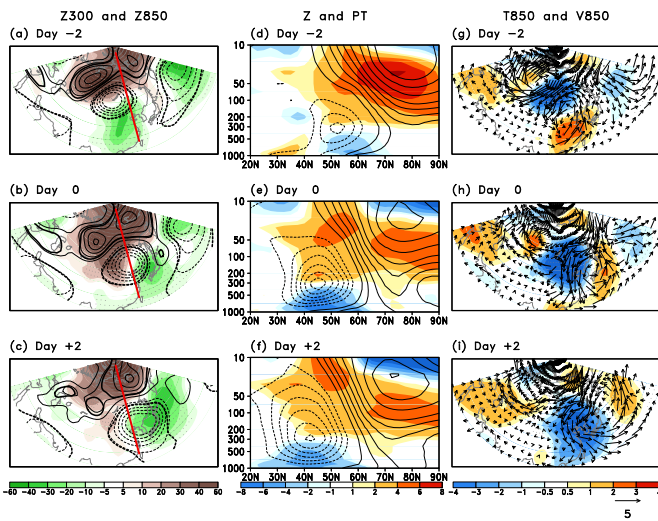

Fig. 4. Same as in Fig. 3, but for 60 cold-surge occurrences during positive AO.